



Original Research Article

Evaluating performance of *malva sylvestris* leaf extract for protection of mild steel against corrosion in acidic solution

Nasrin Soltani^{a,*}, Maryam Khayatkashani^{b,c}

^a Department of Chemistry, Payame Noor University, P.O. Box 19395-3697, Tehran, Iran

^b Research and Development department, Talae Sabz Tuba Pharmaceutical, Tehran, Iran

^c School of Traditional Medicine, Tehran University of Medical Sciences, Tehran, Iran

ARTICLE INFORMATION

Received: 18 August 2019

Received in revised: 16 December 2019

Accepted: 12 January 2020

Available online: 16 March 2020

DOI: 10.22034/ajgc.2021.104987

KEYWORDS

Green corrosion inhibitor

Malva Sylvestris leaf extract

Electrochemical impedance spectroscopy

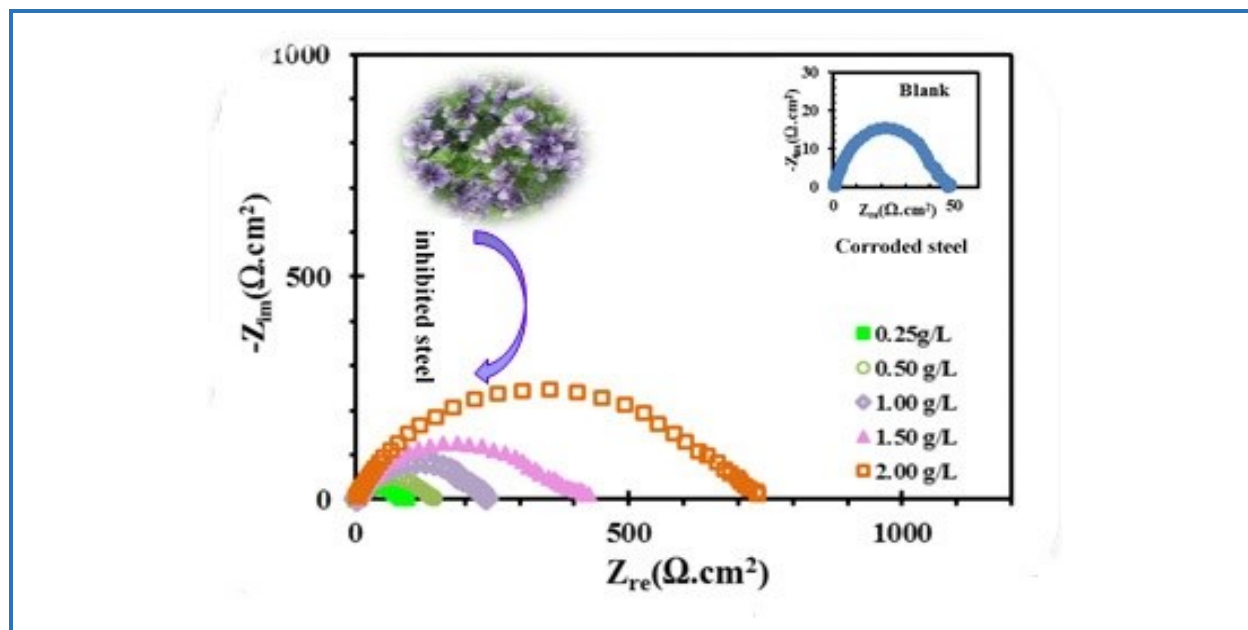
Potentiodynamic polarization

ABSTRACT

In this study, *Malva sylvestris* (*M. sylvestris*) leaf extract was evaluated for the protection surface of the mild steel in 2.0 M HCl solution. For this purpose, the classical method of weight loss and electrochemical methods potentiodynamic polarization and electrochemical impedance spectroscopy (EIS) were used in the first step to assess the performance of the extract. The results showed that, by changing the concentration of the extract from 0.25 g/L to 2.0 g/L in 2.0 M HCl solution, percent inhibition increased from 47% to 93% (for the concentration of 2.0 g/L). In addition, no significant change in the percentage of inhibition was observed as the concentration of the extract exceeded 2.0 g/L. The effect of the temperature on the behavior of the extract, for concentrations of 0.25, 0.5, 1.0, 1.5, and 2.0 g/L, at 35, 45, 55, and 65 °C, were also investigated using polarization method. The percentage of inhibition and coverage were calculated to obtaining the kinetic parameters. The results revealed that, the absorption of molecules of the extract on the surface of the steel obeyed from the Langmuir adsorption isotherm and it was a physical adsorption type.

© 2021 by SPC (Sami Publishing Company), Asian Journal of Green Chemistry, Reproduction is permitted for noncommercial purposes.

Graphical Abstract



Introduction

One of the significant challenges and problems that industries are always facing, is the corrosion of materials. Corrosion has always been one of the most expensive issues facing small and large industries. The phenomenon of corrosion causes energy and capital waste. On the other hand, acids are used in some industries for cleaning the ferrous metals and metal surface degradation in the chemical, petroleum, and nuclear industries, which in turn causes corrosion. Corrosion inhibitors are substances that reduce the rate of corrosion by affecting the cathodic and anodic reactions. These materials are active at low concentrations, and their performance is to form a thin adsorbent layer on the metal surface or to form a protective film. Despite a large number of inhibitors, to select a suitable inhibitor, some points should be taken into account. Toxicity of the inhibitor may have adverse effects on the living things. Also, when the inhibitors are expensive or require a lot of them, their economic value must be considered. Availability of the inhibitor would be an option, because it would be expensive if not available. It should also be environmentally friendly so that the development of non-toxic and non-harmful environmental inhibitors has been widely considered. Many synthetic compounds have been reported as corrosion inhibitors [1–5]. Although synthetic compounds have excellent anti-corrosion properties, most of them are highly toxic to the environment and human life. The toxic effects of synthetic compounds have led to the replacement of natural products as anti-corrosive substances [6–14]. Plant extracts have a wide range of corrosion inhibitors due to their excellent environmental potential, easy access, and renewable resources.

Glycyrrhiza glabra leaves extract [9], red apple fruit extract [15], orange peel extract [16], *Pimenta dioica* leaf extract [17], Egyptian licorice extract [18], and Bamboo leaf extract [18] are some natural inhibitors which have been studied in recent years. *Malva Sylvestris* (*M. sylvestris*) is a species of the mallow genus *Malva* in the family of Malvaceae. It is one of the native and medicinal herbs of Iran that has high nutritional and medicinal value and is used in the treatment of many diseases in traditional Iranian medicine [19]. This plant is found in various region of Iran including, Mazandaran, Hamedan, Lorestan, Isfahan, Fars, Kerman, Tehran, Qazvin, Khorasan, and Sistan provinces. *M. sylvestris* is antibacterial, antidysenteric diaphoretic, pectoral, emollient, mucilaginous, laxative, antitussive, pectoral, and anti-inflammatory. Infusion is used for coughs and colds, irritation of the bronchi, and phagocyte stimulant. This plant has antioxidant, antimicrobial, antiviral, and antinociceptive properties and has been shown to improve the inflammation in laboratory studies. The main constituents are phenolic and flavonoid compounds and the presence of sulphated flavonol glycosides, malvidin 3-glucoside, malvidin 3,5-diglucoside, malvidin 3-(6-malonylglucoside)-5-glucoside, delphinidin 3-glucoside, cyanidin, petunidin, cyanine, beta-carotene, tannins, saponins, alkaloids, mucilage, ascorbic acid and especially antioxidants [19–21]. The present study reviews recent findings of this medicinal plant as corrosion inhibitor.

Experimental

Materials and methods

The mild steel piece with a composition element (wt%): 0.027% C, 0.068% Al, 0.0027% Si, 0.009% P, 0.007% S, 0.007% Cu, 0.340% Mn, 0.003% V, 0.030% Ni, 0.003% Ti, 0.003% Nb, 0.008% Cr and the residue iron, was utilized in this study. The pieces with dimensions 1×1×0.2 cm³, which were employed in the weight loss tests and the pieces which sealed with epoxy resin (exposure surface of 1 cm²), were employed in the electrochemical tests. Before all tests, the mild steel pieces were abraded by emery papers with grades 240, 400, 800, 1000 and 1200, respectively. Then, washed in distilled water, degreased in acetone and at the end dried. 2 M HCl solution was prepared from the HCl with the analytical grade of 37% by using double distilled water.

For the preparation of alcoholic extract of the plant, aerial parts of the *M. sylvestris* were collected from the flowering stage in mid-spring from Isfahan, Iran. The macroscopic and microscopic characteristics of the plant were studied in the anatomy department of the tuba institute of pharmacognosy. 200 g of powdered aerial parts of the *M. sylvestris* was extracted with ethanol and water (70:30, 48 h by percolator) at room temperature. The fractions were concentrated by a rotary evaporator at 40 °C and dried by using a speed vacuum dryer or a freeze dryer and saved at -4 °C. The

yield of *M. sylvestris* extract was found to be 17.2% in ethanol/water solvent with cold extraction. The concentration of *M. sylvestris* extract, which used in this study, was varied from 0.25 to 2.5 g/L⁻¹.

Weight loss measurements were carried out by hanging mild steel pieces in 50 mL of 2 M HCl and 2.0 M HCl containing different concentrations of *M. sylvestris* extract for different immersion times of 2, 4, 8 and 24 h. After these times, the pieces were exited from the beaker, washed carefully by tap and distilled water, respectively. Then, dried and eventually, weighed by using a digital balance with accuracy ± 0.1 mg.

A three-electrode cell assembly involving mild steel electrode, platinum sheet electrode, and a saturated (3 M KCl) silver-silver chloride (Ag/AgCl) electrode as working, counter, and the reference electrode, respectively, and containing 50 mL of electrolyte was utilized for electrochemical tests. Potential-time, potentiodynamic polarization, and EIS analysis were attained by using the Autolab Pgstat 35 model potentiostat-galvanostat. Before conducting the EIS and polarization analysis, the mild steel electrodes were plunged into the solution for 60 min at the OCP (open-circuit potential). For potentiodynamic polarization tests, the potential was scanned from -500 to +500 mV relative to the E_{OCP} , and the scan rate was 0.5 mV/s⁻¹. Polarization parameters such as I_{corr} (corrosion current density) were attained by using GPES electrochemical software through the Tafel extrapolation method. EIS measurements were performed at E_{OCP} after 60 min of immersion time, by a signal amplitude perturbation of 5 mV and in the frequency range of 100 kHz to 0.1 Hz. EIS data were obtained by using FRA software. A scanning electronic microscope (SEM, Philips model XL30) was used to evaluate the surface morphology of the mild steel.

Results and Discussion

Weight loss results

From weight loss measurements, corrosion rate (v), inhibition efficiency ($\eta_w(\%)$), and surface coverage (θ) were calculated using equations 1-3, respectively.

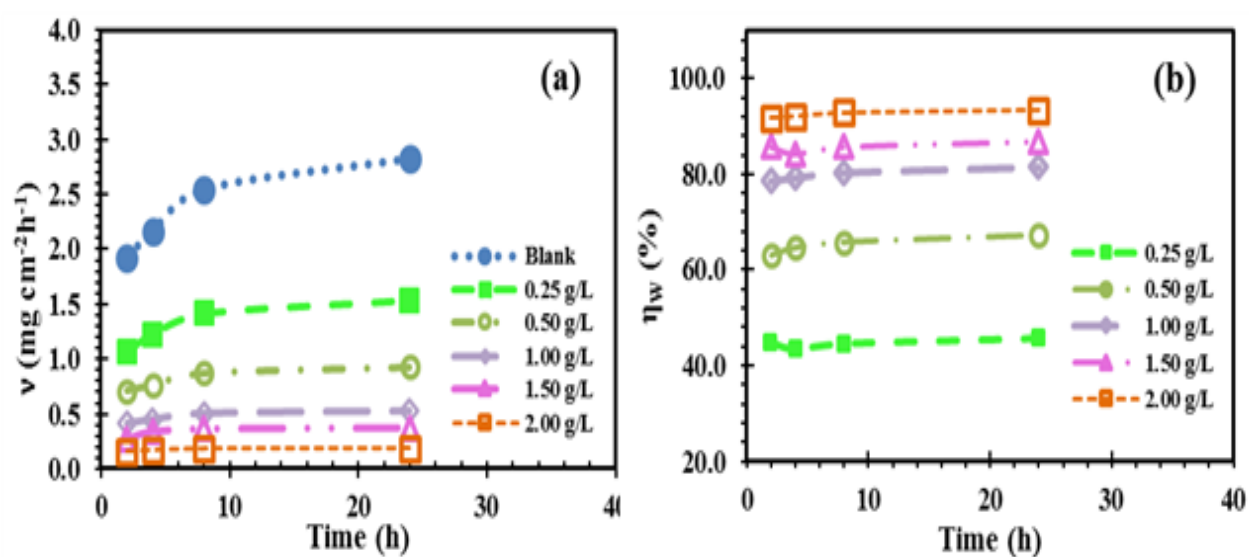
$$v = \frac{(m_1 - m_2)}{(S \times t)} \quad (1)$$

$$\eta_w(\%) = \frac{(v_0 - v)}{v_0} \times 100 \quad (2)$$

$$\theta = \frac{\eta_w(\%)}{100} = \frac{(v_0 - v)}{v_0} \quad (3)$$

Table 1. Corrosion parameters for mild steel in 2.0 M HCl solution in the presence and absence of different concentrations of *M. sylvestris* extract obtained from weight loss for 2 h at 25 °C

Concentration (g/L ⁻¹)	v (mg/cm ² /h ⁻¹)	η_w (%)	θ
Blank	1.92	-	-
0.25	1.06	44.8	0.448
0.50	0.71	63.2	0.632
1.00	0.41	78.5	0.785
1.50	0.27	85.7	0.857
2.00	0.16	91.8	0.918
2.50	0.16	91.7	0.917

**Figure 1.** Relationship between a) corrosion rate (v) and b) inhibition efficiency (η_w) with the immersion time in the absence and presence of different concentrations of *M. sylvestris* extract in 2 M HCl at temperature 25 °C

Where m_1 and m_2 are the mass of the mild steel piece before and after corrosion, respectively, S is the total area of the mild steel piece, t is corrosion time, v_0 and v are the corrosion rates of the pieces in 2.0 M HCl solutions without and with addition of *M. sylvestris* extract, respectively. Table 1 shows the calculated values of v , θ , and η_w values evaluated using equation 1 to equation 3, respectively. To certify the reproducibility of the method, the experiments were performed triplicate, and the average value was reported (Table 1). The results of Table 1 displayed that v decreased with increasing the

M. sylvestris extract, and η_w enhanced with rising the *M. sylvestris* extract concentration. This performance was owing to increasing the adsorption of the molecules in the extract on the surface by increasing the *M. sylvestris* extract concentration. The results also demonstrated that, when the concentration of *M. sylvestris* extract reached about 2.0 g/L⁻¹, the η_w (%) reaches a certain value the remained relatively unchanged (last row of [Table 1](#)).

To evaluate the constancy of the inhibition performance of the *M. sylvestris* extract on the time scale, weight loss tests were conducted in 2.0 M HCl solution without and with various concentrations of the *M. sylvestris* extract for 2–24 h immersion time. [Figure 1a](#) illustrates the v -time curves and [Figure 1b](#) shows the η_w %-time for mild steel corrosion at 25 °C.

As seen in [Figure 1a](#), the v was reduced at the presence of the *M. sylvestris* extract compared with that of the free acid solution. This is testified to this reality that *M. sylvestris* extract practically inhibited the corrosion of the mild steel in 2 M HCl solution. A scan be seen in [Figure 1b](#), by increasing the immersion time from 2 to 24 h, the η_w (%) of *M. sylvestris* extract in all tested concentrations did not display any remarkable change.

Open circuit potential (E_{OCP})

Before each electrochemical test, the electrode immersed in the corrosive test solution to the surface of electrode reaches the steady-state. As demonstrated in [Figure 2](#), after about 1000 s immersion, the E_{OCP} reached a constant value in 2.0 M HCl without and with the *M. sylvestris* extract. Moreover, by addition of the *M. sylvestris* extract to the corrosive media, the E_{OCP} value shifted towards negative and positive values at 0.25 and 2.0 g/L of *M. sylvestris* extract, and there was not a particular relation between E_{corr} and *M. sylvestris* extract concentration. When the displacement in the potential in the presence of the inhibitor relative to in the absence of the inhibitor is at least 85 mV, a inhibitor classified as a cathodic or anodic type [22]. The most significant movement presented by the *M. sylvestris* extract in HCl solution relative to the blank solution was 25 mV. Therefore, it may be deduced that *M. sylvestris* extract performed as a mixed-type inhibitor in HCl media.

Electrochemical impedance spectroscopy (EIS) analysis

Immediately after the E_{OCP} test, an EIS test was performed to evaluate the effect of the *M. sylvestris* extract on the electrode surface. [Figure 3a](#) demonstrates the Nyquist plots of the mild steel in 2.0 M HCl solution without (inset Figure) and with *M. sylvestris* extract. The Nyquist spectra for all the plots, demonstration one single depressed semicircle that their center is under the real axis. The diameter of semicircle increased by rising the concentration of *M. sylvestris* extract, indicating the strengthening of the protective film. Depression is the feature of solid electrodes that attributed to

inhomogeneity and roughness of the surface throughout corrosion [23]. The results of EIS were fitted by using the electrical equivalent circuit in Figure 3b that consists of R_s , R_{ct} , and CPE, represent the solution resistance, charge transfer resistance, and constant phase element (instead of the double layer (C_{dl})), respectively. The impedance (Z) of CPE was calculated using the equation 4 [24].

$$Z_{CPE} = Q^{-1}(j\omega)^{-n} \tag{4}$$

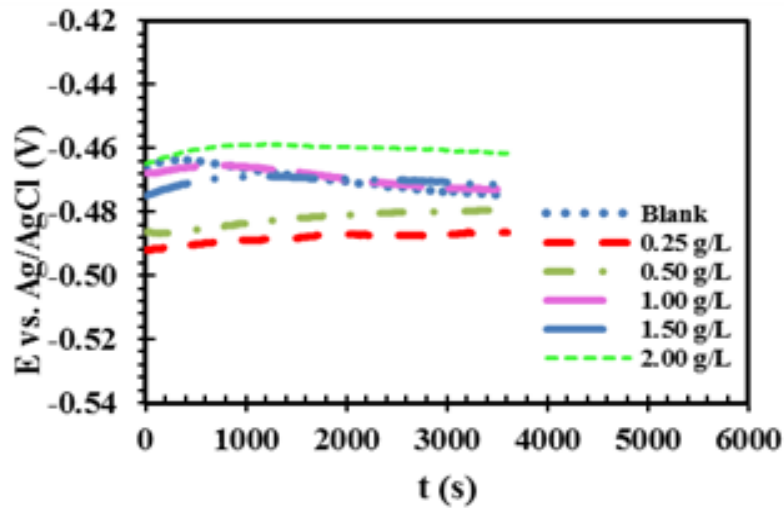


Figure 2. OCP plots for mild steel in 20 M HCl in the absence and presence of different concentration of *M. sylvestris* extract

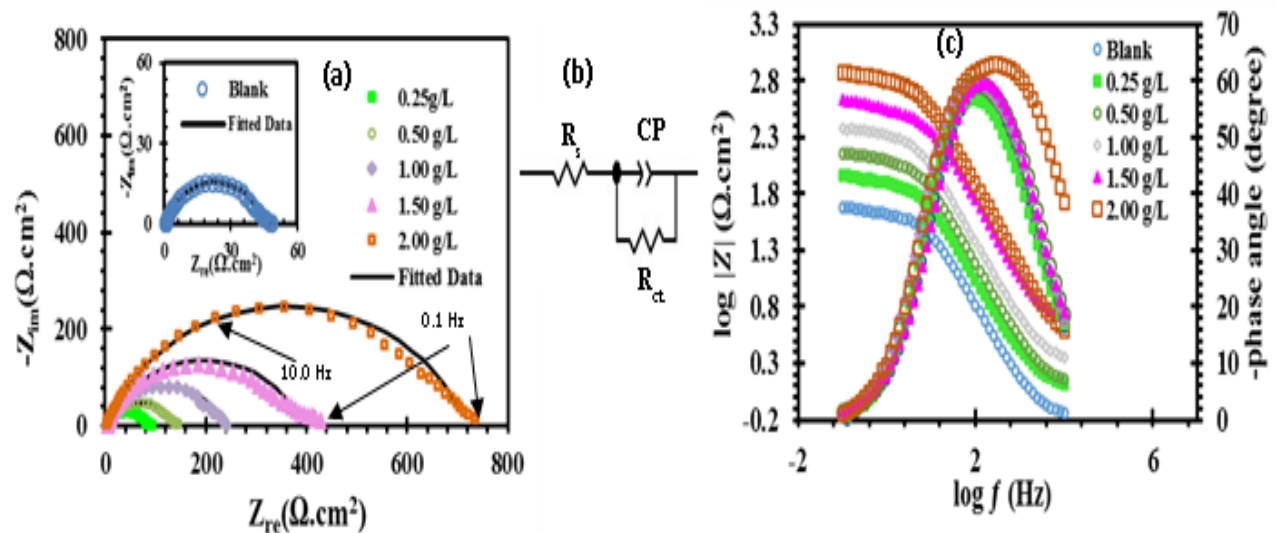


Figure 3. a) Nyquist plots, b) electrical equivalent circuit model used to fit impedance data and c) Bode and phase angle plots for mild steel in 2 M HCl in the absence and presence of different concentration of *M. sylvestris* extract

Table 2. Impedance data of mild steel in 2 M HCl with and without *M. sylvestris* extract

Concentration (g/L ⁻¹)	R _s (Ω/cm ²)	R _{ct} (Ω/cm ²)	CPE		η _{EIS} (%)
			Q (μΩ ⁻¹ /s ⁿ /cm ⁻²)	n	
Blank	0.5	45.2	1022.3	0.77	-
0.25	0.8	86.7	309.2	0.80	47.8
0.50	1.2	138.7	153.4	0.82	67.4
1.00	1.6	235.6	144.6	0.83	80.8
1.50	2.3	386.5	59.1	0.84	88.3
2.00	2.7	714.7	38.5	0.85	93.6

Where Q is the CPE constant, ω is the angular frequency, $j^2 = -1$ is the imaginary number and n representation the degree of surface inhomogeneity subsequent surface roughness, inhibitor adsorption, and porous layer formation. The results are listed in Table 2. The chi-square (χ^2) varied in the range of 0.0034 to 0.005588, which represents accurate fitting of the data. These results illustrate that R_{ct} enhanced with increasing the concentration of the *M. sylvestris* extract. It displayed the improved protection effects of *M. sylvestris* extract and reduce the corrosion rate. This was basically due to reducing the number of active sites of corrosion reaction because of the replacement of water molecules on the surface with extract molecules [9]. The Q values decreased with increasing the extract concentration. This can be associated with the increased thickness of the double layer and, or reduced dielectric constant [25]. The decreased Q values recommended the decreased thickness of the oxide layer of surface and the effect of the electrode procedure on the kinetics according to the changed oxide layer in the presence of extract molecules [9]. The lower value of n for 2.0 M HCl solution show inhomogeneity of surface as a result of the roughening of metal surface owing to corrosion. The increase in the amount of n value is due to the decrease of the surface inhomogeneity owing to the adsorption of the extract molecules.

The inhibition efficiencies ($\eta_{EIS}\%$) at different extract concentrations were obtained by using the equation (5):

$$\eta_{EIS}\% = \frac{R_{ct(inh)} - R_{ct}}{R_{ct(inh)}} \times 100 \quad (5)$$

Where R_{ct} and $R_{ct (inh)}$ are the resistance of charge transfer without and with *M. sylvestris* extract, respectively. The η_{EIS} (%) obtained from the EIS method are run parallel with η_w (%) values. In the Bode plots (Figure 3c), the absolute impedance increased with increasing the concentration of the extract at lower frequencies due to the adsorption of the molecules of the extract onto the steel surface [26]. From the phase angle plots (Figure 3c), it can be seen that only one phase peak near -90° was visible at the middle frequency. It indicated that, there is only one time constant ($R_{ct} C_{dl}$) for inhibited and uninhibited solutions. As the concentration of the extract in solution increased, the phase angle shifted to negative values, indicating better absorption of the extract molecules onto the metal surface with increasing the concentration [27].

Potentiodynamic polarization measurements

Figure 4 illustrates the potentiodynamic polarization curves of the mild steel in 2.0 M HCl without and with various concentrations of *M. sylvestris* extract. As seen in Figure 4, both the anodic and cathodic branches showed a lower current density at the presence of the *M. sylvestris* extract relative to 2.0 M HCl solution. This performance indicated that the *M. sylvestris* extract affects both the anodic and cathodic reactions in the process of corrosion. The electrochemical parameters such as I_{corr} , corrosion potential (E_{corr}), and anodic and cathodic Tafel slopes (b_c and b_a) attained from the polarization curves, and also inhibition efficiency ($\eta_{pol}\%$), obtained from equation 6, for different extract concentrations are listed in Table 3.

$$\eta_{pol}(\%) = \left(\frac{I_0 - I}{I_0} \right) \times 100 \quad (6)$$

I and I_0 are the corrosion current densities in the presence and absence of *M. sylvestris* extract, respectively.

As shown in Table 3, increasing the concentration of the *M. sylvestris* extract raised the $\eta_{pol}\%$ and reduced the I_{corr} . This shows the ability of the *M. sylvestris* extract to prevent the corrosion of the mild steel in HCl solution. Regarding the potentiodynamic polarization curves, the E_{corr} values changed slightly to the more positive potentials with the addition of *M. sylvestris* extract. However, there was not a particular relation between the E_{corr} and concentration of the *M. sylvestris* extract. It may be related to the adsorption of the compound of *M. sylvestris* extract on the active sites of the electrode surface and delaying the corrosion reaction [28]. There was also no significant change in the b_c and b_a Tafel slopes. The approximately constant values of cathodic and anodic Tafel slopes suggested that the *M. sylvestris* extract did not change the mechanism of the hydrogen evolution reaction and iron

dissolution, respectively. This means that the inhibition action of the *M. sylvestris* extract was related to only blocking the reaction sites of the steel surface [28].

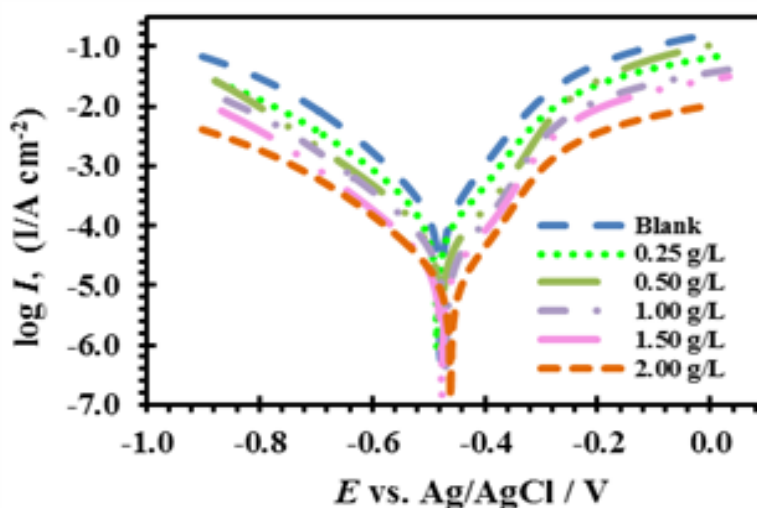


Figure 4. Polarization curves for the mild steel in 2 M HCl with different concentration of *M. sylvestris* extract

Table 3. Polarization parameters for mild steel in 2 M HCl in the presence and absence of *M. sylvestris* extract

Concentration (g/L ⁻¹)	$-E_{corr}$ (V/vs. Ag/AgCl)	$-b_c$ (V/dec ⁻¹)	b_a	I_{corr} ($\mu\text{A}/\text{cm}^2$)	θ	η_{pol} (%)
Blank	-0.479	103	89	132.2	-	-
0.25	-0.474	100	120	87.4	0.339	33.89
0.50	-0.477	95	116	41.2	0.688	68.84
1.00	-0.470	108	112	28.9	0.781	78.14
1.50	-0.476	96	104	14.9	0.887	88.73
2.00	-0.461	99	89	9.4	0.929	92.89

Effect of temperature and activation parameters

To estimate the stability of the adsorbed layer on the steel surface and also to obtain activation parameters, potentiodynamic polarization experiments were carried out in the range of 35–65 °C without and with different concentrations of *M. sylvestris* extract during 2 h immersion time. Figure 5 shows the resulting polarization curves, and the obtained parameters are shown in Table 4.

As seen in Table 4, by increasing temperature, I_{corr} increased and the inhibition efficiency decreased. Decreasing the $\eta_{pol}\%$ by increasing the temperature was due to the increased rate of the

dissolution of mild steel and fractional desorption of the compound of *M. sylvestris* extract from the surface with increasing temperature [29]. To calculate the activation parameters, equation 7 (Arrhenius equation) and equation 8 (transition state equation) were used [30].

$$r = \lambda \exp\left(\frac{-E_a}{RT}\right) \quad (7)$$

$$r = \frac{RT}{N_A h} \exp\left(\frac{\Delta S^*}{R}\right) \exp\left(-\frac{\Delta H^*}{RT}\right) \quad (8)$$

Where r is the rate of metal dissolution reaction (directly related to I_{corr}), λ is the Arrhenius pre-exponential factor, E_a is the activation corrosion energy for the corrosion process, T is the absolute temperature, h is the planck's constant, N_A is the Avogadro's number, ΔS^* and ΔH^* are the entropy and enthalpy of activation, respectively [31].

The apparent activation energy (E_a) of the corrosion reaction in corrosion media can be calculated by plotting $\ln I_{\text{corr}}$ with $1/T$. From this curve, the straight line is obtained, which E_a can be calculated from its slope. The Arrhenius curves without and with the addition of various concentrations of *M. sylvestris* extract are represented in Figure 6a. The obtained values of E_a are listed in Table 5 show that the values of E_a obtained in solutions containing *M. sylvestris* extract are higher than the E_a of HCl 2.0 M solution. These results may be explicated as physical adsorption that happens in the first stage [32]. Szauer and Brand [33] explicated that the increase in E_a can be attributed to a considerable reduction in the adsorption of the inhibitor on the surface by the increase of temperature.

By plot of $\ln(I_{\text{corr}}/T)$ against $1/T$ gain a straight line with the slope and intercept equal to $(-\Delta H^*/R)$, and $[\ln(\frac{R}{Nh}) + (\frac{\Delta S^*}{R})]$, respectively, as shown in Figure 6b. From these plots, ΔH^* and ΔS^* were obtained and are demonstrated in Table 5. The positive signs of ΔH^* in Table 5 reverberate the endothermic nature of steel dissolution procedure and concepting that the dissolution of steel is complicated [29]. From Table 5, it is considered that E_a and ΔH^* values change in the same manner. This result permits to investigate of the recognized thermodynamic reaction between the E_a and ΔH^* ($E_a - \Delta H^* = RT$). The calculated values are close to RT (2.48 kJ/mol at 298 K). The negative values of ΔS^* indicate that the activated complex tends to associate more than dissociation, in the rate-determining step. Therefore, when going from reactants to the activated complex, a decrease in disordering occurred [34].

Adsorption isotherm

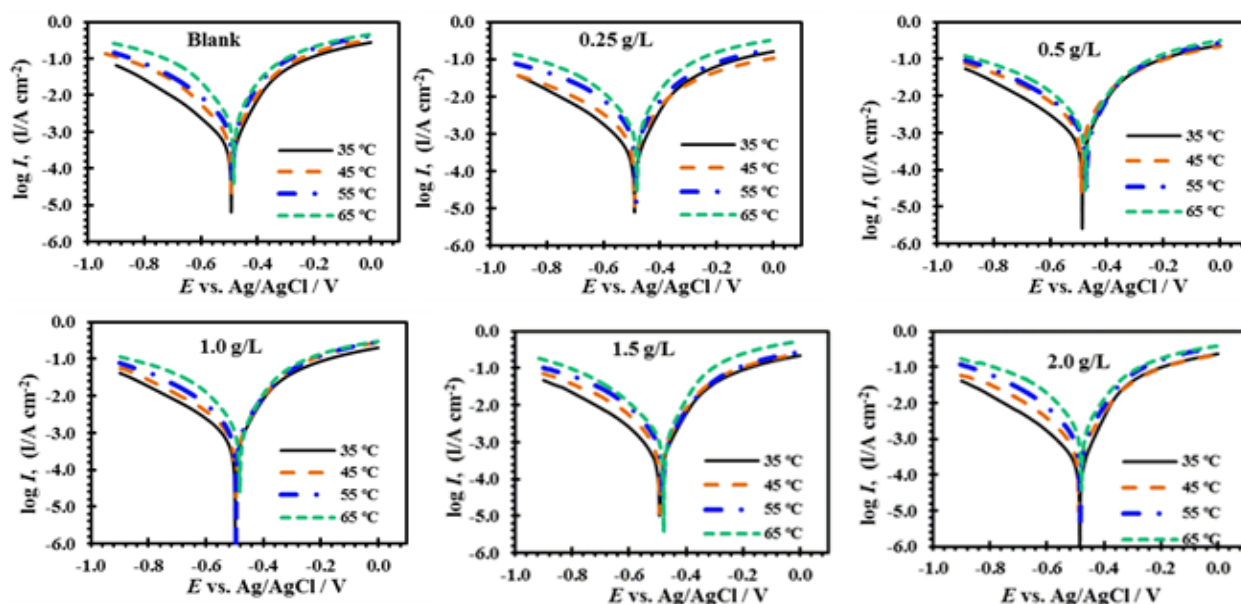


Figure 5. Effect of temperature on polarization curves of mild steel corrosion rate in free (2 M HCl) and inhibited acid solutions

Table 4. Polarization parameters and corresponding inhibition efficiency for the corrosion of the mil steel in 2 M HCl with and without *M. sylvestris* extract at different temperatures

Temperature (°C)	Concentration (g/L ⁻¹)	$-E_{corr}$ (V/ vs. Ag/AgCl)	$-b_c$ (V/dec ⁻¹)	b_a (V/dec ⁻¹)	I_{corr} (μA/cm ⁻²)	θ	η_{pol} (%)
35	Blank	530	175	86	552.0	-	-
	0.25	490	137	83	299.2	0.458	45.80
	0.50	487	160	77	198.4	0.641	64.06
	1.00	498	139	80	122.1	0.779	77.88
	1.50	493	204	97	87.3	0.842	84.18
	2.00	485	120	73	52.7	0.905	90.45
45	Blank	492	133	94	1130.0	-	-
	0.25	490	158	102	638.7	0.435	43.48
	0.50	490	162	103	426.3	0.623	62.27
	1.00	496	139	94	282.4	0.750	75.01
	1.50	491	127	99	195.9	0.827	82.66
	2.00	487	120	93	133.7	0.882	88.17
55	Blank	489	122	78	1924.0	-	-
	0.25	485	131	107	1117.0	0.419	41.94
	0.50	472	136	88	788.6	0.590	59.01

	1.00	495	125	100	521.3	0.729	72.91
	1.50	481	122	106	398.6	0.793	79.28
	2.00	483	115	93	390.5	0.797	79.70
65	Blank	485	114	78	2414.0	-	-
	0.250	481	265	118	1449.0	0.400	39.98
	0.50	474	163	101	1022.4	0.576	57.65
	1.00	482	102	85	726.0	0.699	69.93
	1.50	478	135	85	549.9	0.772	77.22
	2.00	478	107	93	539.7	0.776	77.64

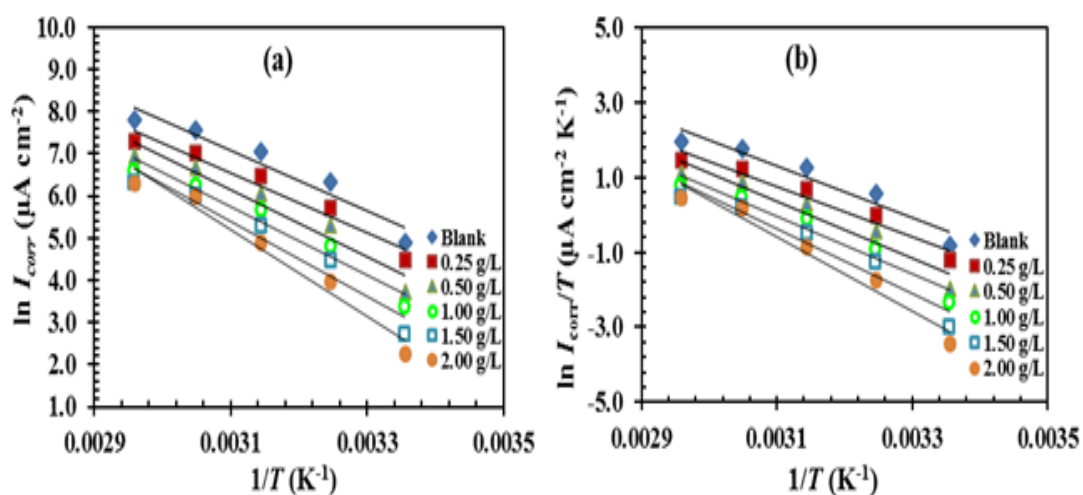


Figure 6. Arrhenius plots of a) $\ln I_{\text{corr}}$ versus $1/T$ and (b) $\ln (I_{\text{corr}}/T)$ versus $1/T$ in the absence and presence of different concentration of *M. sylvestris* extract in 2 M HCl

Table 5. Activation parameters, E_a , ΔH^* , ΔS^* , of the dissolution of mild steel in 2 M HCl in the absence and presence of *M. sylvestris* extract

Activation parameters	Concentration (g/L ⁻¹)					
	Blank	0.25	0.50	1.00	1.50	2.00
E_a (kJ/mol ⁻¹)	58.58	59.74	66.03	66.74	73.89	85.24
ΔH^* (kJ/mol ⁻¹)	55.95	57.11	63.39	64.11	71.25	82.61
ΔS^* (J/mol ⁻¹ /K ⁻¹)	-9.66	-17.73	-1.96	-0.88	20.21	-53.69

The adsorption isotherm describes the adsorption behavior of the organic compounds to better understand the adsorption mechanism. Various adsorption isotherms such as Langmuir, Temkin, Freundlich, Bockris–Swinkels and Flory–Huggins isotherms can be used to distinguish the

adsorption action of the inhibitors. Langmuir adsorption isotherm, which defined by equation 9 was established to be the best fit from all of the examined isotherms. The R² (correlation coefficient) value was utilized as a criterion to conclude the best fit adsorption isotherm.

$$\frac{C_{inh}}{\theta} = \frac{1}{K_{ads}} + C_{inh} \quad (9)$$

Where (C_{inh}) is the extract concentration, θ is the degree of coverage of surface and K_{ads} is the equilibrium constant of adsorption–desorption procedure. The inhibition efficiency (η_{pol}) as $\theta = \eta_{pol}/100$ from potentiodynamic polarization data was used for the estimate of the θ for different concentrations at various temperatures. The relationship between C/ θ and C at different temperatures is shown in Figure 7. The obtained plots are linear, with the slope nearly to unity. According to this isotherm, the adsorbed molecules present in the *M. sylvestris* extract occupy only one site and as well as, there are no interactions between adsorbed species [35]. The K_{ads} at 25, 35, 45, 55 and 65 °C are 2.38, 3.22, 3.01, 3.29 and 2.99, respectively.

The K_{ads} is related to the standard adsorption free energy (ΔG^0_{ads}) according to equation 10 [36]:

$$K_{ads} = \left(\frac{1}{55.5}\right) \exp\left(\frac{-\Delta G^0_{ads}}{RT}\right) \quad (10)$$

Where R and T are the gas constant and absolute temperature of the experiment, respectively. The constant value of 55.5 is the concentration of water in solution in mol/dm⁻³. According to scientist's view, values of ΔG^0_{ads} up to -20 kJ/mol⁻¹ are following physical absorption means the electrostatic interaction between the charged molecules and the oppositely charged metal occurs. While ΔG^0_{ads} more negative than about -40 kJ/mol⁻¹ are following chemisorption means sharing or transfer of electrons from the inhibitor molecules to the metal surface is occurred to form a coordinate bond [37]. However, due to the unknown average molecular mass and the complex composition of the *M. sylvestris* extract, calculation of ΔG^0_{ads} was not possible. Therefore, evaluating the adsorption behavior of the *M. sylvestris* extract by using the ΔG^0_{ads} was impossible [38].

SEM analyses

To assess the condition of mild steel surface in contact with HCl solution, SEM images after 24 h immersion in 2.0 M HCl solution containing the most effective concentration of *M. sylvestris* extract at 25 °C was taken (Figure 8). SEM image of the abraded surface of mild steel before being placed in the test solution is shown in Figure 8a. In this Figure, the lines created during the abrading of the

surface are seen in the image. **Figure 8b** shows the severe degradation of the surface of mild steel in the HCl solution compared to **Figure 8a**. **Figure 8c** illustrates the ability of the *M. sylvestris* extract to protection mild steel in the 2 M HCl medium containing 1 g/L of the *M. sylvestris* extract, which confirms the formation of a protective film on the surface of mild steel.

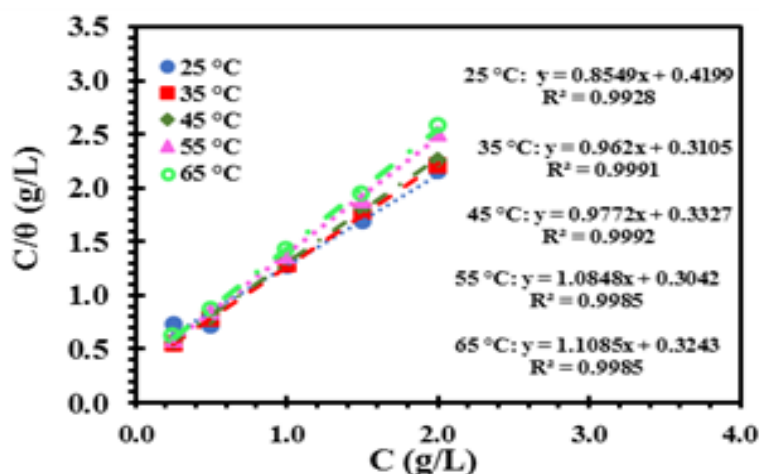


Figure 7. Langmuir isotherm for adsorption of *M. sylvestris* extract in 2 M HCl solution on the mild steel surface

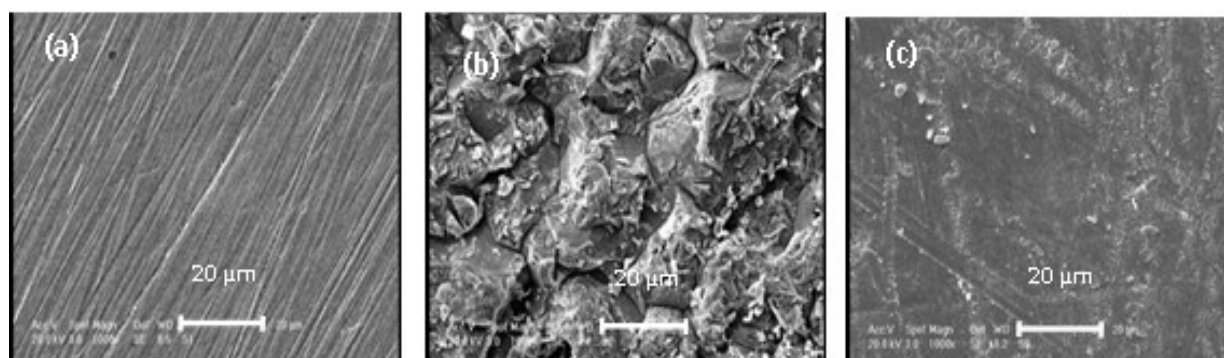
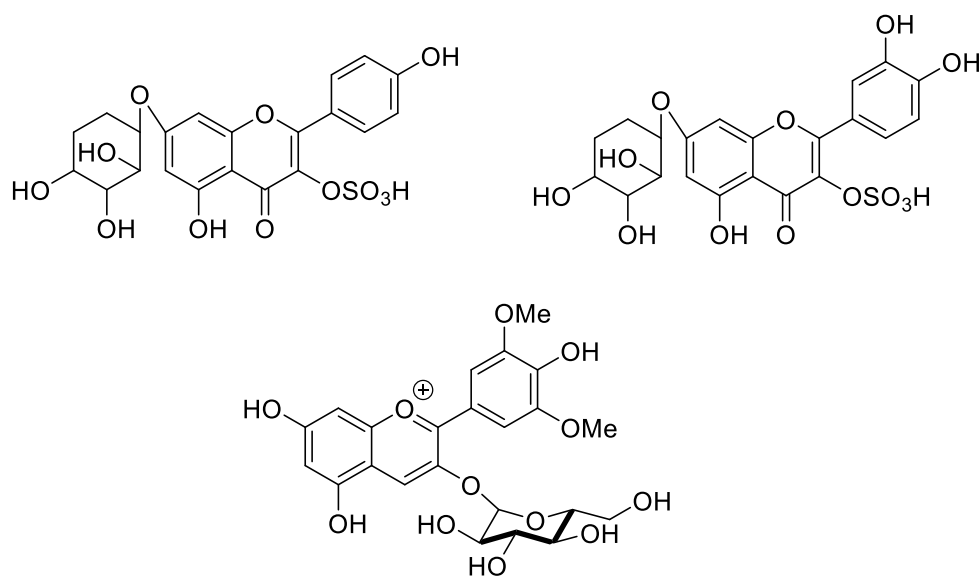


Figure 8. SEM micrographs of mild steel samples, a) before corrosion, and after 24 h immersion in b) 2 M HCl, and c) 2 M HCl containing 2 g/L extract

Adsorption mechanism

In this study, the results of the investigation of the inhibitory influence of *M. sylvestris* extract on the metal of mild steel surface showed that by increasing the extract concentration, the inhibition percentage increased. Therefore, it can be concluded that as the concentration of the extract increased, the number of extract molecules adsorbed on the metal surface increased, and therefore, the fraction of the metal surface that was directly attacked by the acid decreased. The first stage in the mechanism action of the inhibitors is their adsorption onto the metal surface. In most studies of

corrosion inhibitors, the formation of donor-acceptor complexes between π electrons of the inhibitor and the d -orbitals of metal is accepted. Based on Scheme 1, the main constituents of *M. sylvestris* extract [19–21] contain OH functional group and a large number of aromatic rings that protonated in hydrochloric acid medium. On the other hand, the mild steel surface charge in hydrochloric acid medium is reported to be positive [39]. As a result, in HCl solution, Cl^- anions are first adsorbed to the metal surface, and surface is negatively charged to the solution, and conditions are provided for the adsorption of protonated compounds onto the surface. In other words, there is a synergistic effect between the anion (Cl^-) and the positive charge compounds that present in the solution. Upon adsorption of the protonated molecules of the extract onto the metal surface, a coordinate bond is formed by electron transfer from the oxygen atoms and π electrons of the aromatic rings of the organic molecules of the extract to iron- d orbitals. The free pair's electrons of oxygen atoms in the extract compounds may be combined with Fe^{2+} ions formed on the metal surface to form metal-inhibitor complexes.



Scheme 1. The structure of the some major constituents found in *M. sylvestris* extract

Conclusions

M. sylvestris extract is a suitable inhibitors for mild steel in 2.0 M HCl. The inhibition efficiency increases with increasing extract concentration. The values of $\eta\%$ for *M. sylvestris* extract compared with the results of some other extracts in Table 6. The $\eta\%$ of *M. sylvestris* extract was found to be higher than the *Glycyrrhiza glabra* extract, red apple fruit extract, Egyptian licorice, and Bamboo leaf extract. But, $\eta\%$ is lower than orange peel extract, pimenta dioica leaf extract and *Salvia officinalis* leaves extract. This difference in behavior may be due to differences in the type of metal and corrosive

Table 6. Comparison of *M. sylvestris* extract results with other reported extract as inhibitor

Extract	Type of metal	Type of solution	Concentration	Maximum efficiency	Ref
Glycyrrhiza glabra extract	Mild steel	1 M HCl	800 ppm	88%	[9]
Red apple (Malus domestica) fruit extract	Mild steel	0.5 M HCl	5 g/L	90%	[15]
Orange peel extract	Carbon steel	0.1 M HCl	10% V/V	98%	[16]
Pimenta dioica leaf extracts	Mild steel	0.5 M and 1.0 M HCl	0.13 % V/V	98% and 99%	[17]
Egyptian licorice	Copper	0.1 M HCl	4.0 % V/V	89.5%	[18]
Bamboo leaf extract	Cold rolled steel	1.0 M HCl and 0.5 M H ₂ SO ₄	200 mg/L	90.3% and 79.2%	[37]
Salvia officinalis leaves extract	304 stainless steel	1 M HCl	2 g/L	96.2%	[33]
<i>M. sylvestris</i> extract	Mild steel	2 M HCl	2 g/L	93%	This study

environments. Polarization curves measurements indicated that the *M. sylvestris* extract acted as a mixed type. The inhibition action was due to the adsorption of the *M. sylvestris* extract molecules on the metal and blocking the active sites of the surface. For all of the examined temperatures, the adsorption of the *M. sylvestris* extract was well described by the Langmuir isotherm model. The values of E_a revealed that, the *M. sylvestris* extract was adsorbed by a physisorption process.

Acknowledgments

The financial support of research council of the Payame Noor University of Isfahan and Shahinshahr is gratefully acknowledged.

Disclosure Statement

No potential conflict of interest was reported by the authors.

References

- [1]. Mishra A., Verma C., Lgaz H., Srivastava V., Quraishi M.A., Ebenso E.E. *J. Mol. Liq.*, 2018, **251**:317
- [2]. Luo X., Ci C., Li J., Lin K., Du S., Zhang H., Li X., Cheng Y.F., Zang J., Liu Y. *Corros. Sci.*, 2019, **151**:132
- [3]. Singh A., Ansari K.R., Haque J., Dohare P., Lgaz H., Salghi R., Quraishi M.A. *J. Taiwan Inst. Chem. Eng.*, 2018, **82**:233
- [4]. Sadeghi Erami R., Amirnasr M., Meghdadi S., Talebian M., Farrokhpour H., Raeissi K. *Corros. Sci.*, 2019, **151**:190
- [5]. Saha S.K., Banerjee P. *Mater. Chem. Front.*, 2018, **2**:1674
- [6]. Alibakhshi E., Ramezanzadeh M., Haddadi S.A., Bahlakeh G., Ramezanzadeh B., Mahdavian M. *J. Clean. Produc.*, 2019, **210**:660
- [7]. Sanaei Z., Ramezanzadeh M., Bahlakeh G., Ramezanzadeh B. *J. Ind. Eng. Chem.*, 2019, **69**:18
- [8]. Haddadi S.A., Alibakhshi E., Bahlakeh G., Ramezanzadeh B., Mahdavian M. *J. Mol. Liq.*, 2019, **284**:682
- [9]. Alibakhshi E., Ramezanzadeh M., Bahlakeh G., Ramezanzadeh B., Mahdavian M., Motamedi M. *J. Mol. Liq.*, 2018, **255**:185
- [10]. Ramezanzadeh M., Bahlakeh G., Sanaei Z., Ramezanzadeh B. *J. Mol. Liq.*, 2018, **272**:120
- [11]. Ramezanzadeh M., Bahlakeh G., Sanaei Z., Ramezanzadeh B. *Appl. Surf. Sci.*, 2019, **463**:1058
- [12]. Bahlakeh G., Ramezanzadeh B., Dehghani A., Ramezanzadeh M. *J. Mol. Liq.*, 2019, **283**:174
- [13]. Saxena A., Prasad D., Haldhar R., Singh G., Kumar A. *J. Environ. Chem. Eng.*, 2018, **6**:694
- [14]. Verma C., Quraishi M.A., Ebenso E.E., Bahadur I. *J. Bio Tribo Corros.*, 2018, **4**:33
- [15]. Umoren S., Obot I.B., Gasem Z., Odewunmi N.A. *J. Dispers. Sci. Technol.*, 2015, **36**:789
- [16]. M'hiri N., Veys-Renaux D., Rocca E., Ioannou I., Boudhrioua N.M., Ghoul. M. *Corros. Sci.*, 2016, **102**:55
- [17]. Anupama K.K., Ramya K., Shainy K.M., Joseph A. *Mater. Chem. Phys.*, 2015, **167**:28
- [18]. Deyab M.A. *J. Ind. Eng. Chem.*, 2015, **22**:384
- [19]. Samavati V., Manoochehrizade A. *Int. J. Biol. Macromol.*, 2013, **60**:427
- [20]. Prudente A.S., Loddi A.M.V., Duarte M.R., Santos A.R.S., Pochapski M.T., Pizzolatti M.G., Hayashi S.S., Campos F.R., Pontarolo R., Santos F.A., Cabrini D.A., Otuki M.F. *Food Chem. Toxicol.*, 2013, **58**:324
- [21]. Barros L., Carvalho A.M., Ferreira I.C.F.R. *Food Chem. Toxicol.*, 2010, **48**:1466
- [22]. Ji G., Dwivedi P., Sundaram S., Prakash R. *Res. Chem. Intermed.*, 2016, **42**:439
- [23]. Srivastava M., Tiwari P., Srivastava S.K., Kumar A., Ji G., Prakash R. *J. Mol. Liq.*, 2018, **254**:357
- [24]. Srivastava M., Tiwari P., Srivastava S.K., Prakash R., Ji G. *J. Mol. Liq.*, 2017, **236**:184
- [25]. Bahrami M.J., Hosseini S.M.A., Pilvar P. *Corros. Sci.*, 2010, **52**:2793
- [26]. Tang Y., Zhang F., Hu S., Cao Z., Wu Z., Jing W. *Corros. Sci.*, 2013, **74**:271
- [27]. Xu B., Yang W., Liu Y., Yin X., Gong W., Chen Y. *Corros. Sci.*, 2014, **78**:260
- [28]. Soltani N., Tavakkoli N., Ghasemi M. *Int. J. Electrochem. Sci.*, 2016, **11**:8827
- [29]. Singh A., Ahamad I., Singh V.K., Quraishi M.A. *J. Solid State Electrochem.*, 2011, **15**:1087

- [30]. Saxena A., Prasad D., Haldhar R. *Bioelectrochemistry*, 2018, **124**:156
- [31]. Behpour M., Ghoreishi S.M., Kashani M.K., Soltani N. *Mater. Corros.*, 2009, **60**:895
- [32]. Larif M., Elmidaoui A., Zarrouk A., Zarrok H., Salghi R., Hammouti B., Oudda H., Bentiss F. *Res. Chem. Intermed.*, 2013, **39**:2663
- [33]. Szauer T., Brandt A. *Electrochim. Acta*, 1981, **26**:1253
- [34]. Soltani N., Tavakkoli N., Khayatkashani M., Jalali M.R., Mosavizade A. *Corros. Sci.*, 2012, **62**:122
- [35]. Behpour M., Ghoreishi S.M., Khayatkashani M., Soltani N. *Mater. Chem. Phys.*, 2012, **131**:621
- [36] Soltani N., Salavati H., Rasouli N., Paziresh M., Moghadasi A. *Chem. Eng. Commun.*, 2016, **203**:840
- [37]. Deng S., Li X. *Corros. Sci.*, 2012, **64**:253
- [38]. Wang Q., Tan B., Bao H., Xie Y., Mou Y., Li P., Chen D., Shi Y., Li X., Yang W. *Bioelectrochemistry*, 2019, **128**:49
- [39]. Li X., Deng S., Fu H. *Corros. Sci.*, 2012, **62**:163

How to cite this manuscript: Nasrin Soltani*, Maryam Khayatkashani. Evaluating performance of *malva sylvestris* leaf extract for protection of mild steel against corrosion in acidic solution. *Asian Journal of Green Chemistry*, 5(1) 2021, 39-57. DOI: 10.22034/ajgc.2021.104987